



Trophic ecology of Caribbean octocorals: autotrophic and heterotrophic seasonal trends

Sergio Rossi^{1,2,3,4} · Nadine Schubert^{5,7} · Darren Brown^{5,8} · Alba Gonzalez-Posada⁶ · Marcelo O. Soares^{2,4}

Received: 12 November 2019 / Accepted: 15 February 2020 / Published online: 25 February 2020
© Springer-Verlag GmbH Germany, part of Springer Nature 2020

Abstract Studies over the past decades indicate that octocorals are becoming the dominant group in some areas of the Caribbean. Yet, basic knowledge about the trophic ecology of these organisms and their seasonal and species-specific variability is still scarce, though this might play a key role in determining their importance in benthic–pelagic coupling processes and, consequently, their role in carbon cycles. In the present study, two Caribbean gorgonian species (*Plexaurella nutans* and *Pterogorgia anceps*) were

studied during an annual cycle, to assess seasonal variations in their reliance on heterotrophic versus autotrophic energy inputs. Zooplankton capture rates and bulk tissue stable isotopes were measured on a monthly basis to assess heterotrophic energy input, while autotrophic contribution was quantified monthly by Symbiodiniaceae cell densities and pigment contents, accompanied by seasonal measurements on Symbiodiniaceae (*Breviolum* sp.) photosynthetic performance and host respiratory demand. The results show that while autotrophy was the main energy source for both species, there was also a non-neglectable input through zooplankton that accounted for 0.2–0.8% and 0.7–3.4% of the energy demands in *P. nutans* and *P. anceps*, respectively. Our data further demonstrate that there are species-specific and seasonal differences in the contributions of these two nutrition modes, though there is no indication of shifts in the predominant mode during the year in either species. The energy inputs resulted in a positive energy balance throughout the year, with an energy surplus available for somatic growth, gonads, and/or energy reserves (e.g., lipids). However, the seasonal patterns differed between species, a feature that is most likely related to the different reproduction periods of the octocorals. Altogether, the information gathered here serves for a better understanding of the trophic ecology of mixotrophic octocorals and the seasonal variability of the nutritional modes that will define their potential impact in the carbon cycle and benthic–pelagic coupling processes of coral reefs.

Topic Editor Anastazia Banaszak

Electronic supplementary material The online version of this article (<https://doi.org/10.1007/s00338-020-01906-w>) contains supplementary material, which is available to authorized users.

✉ Sergio Rossi
sergio.rossi@unisalento.it

- 1 DiSTeBA, University of Salento, Lecce, Italy
- 2 The Environmental Science and Technology Institute, Autonomous University of Barcelona, Campus UAB s/n, Barcelona, Spain
- 3 CoNISMa, Consorzio Nazionale Interuniversitario per le Scienze del Mare, Rome, Italy
- 4 Instituto de Ciências do Mar (Labomar), Universidade Federal do Ceará, Fortaleza, Ceará, Brazil
- 5 Unidad Académica de Sistemas Arrecifales Puerto Morelos (ICMyL), Universidad Nacional Autónoma de México (UNAM), Cancún, Mexico
- 6 Comisión Nacional para el Conocimiento y Uso de la Biodiversidad (CONABIO), Mexico City, Mexico
- 7 Present Address: CCMAR - Centre of Marine Sciences, University of Algarve, Campus Gambelas, Faro, Portugal
- 8 Present Address: Department of Biology, The Pennsylvania State University, University Park, PA, USA

Keywords Autotrophic versus heterotrophic input · Benthic–pelagic coupling · Caribbean · Octocoral · Trophic ecology

Introduction

Octocorals are one of the most noticeable organisms in marine benthic communities in both reef environments and soft bottoms, able to inhabit the oceans from the tropics to the polar regions and from the shallow to the deep (Rossi et al. 2017a). In many environments, they play a fundamental role as ecosystem engineers (sensu Jones et al. 1994), providing three-dimensional structures that serve as habitats for hundreds of associated organisms. In addition, by releasing organic matter in the form of mucus and capturing plankton and dissolved organic matter, they play a key role in the transfer of energy and nutrients between the pelagic and benthic systems (Coma et al. 1998; Rossi et al. 2017b). As recently shown for Mediterranean gorgonians, the carbon removal as a consequence of their autotrophic and heterotrophic energetic strategies might represent a not-yet-considered important component of the global carbon cycle (Coppari et al. 2019).

In the tropics, a high proportion of octocoral species in shallow coral reefs are mixotrophic, living in symbiosis with photosynthetic dinoflagellates of the family Symbiodiniaceae (reviewed in Schubert et al. 2017). Despite those species relying greatly on the autotrophic energy input through symbiont photosynthesis, they also have a non-negligible heterotrophic component (Sorokin 1991; Fabricius and Klumpp 1995; Ribes et al. 1998; Baker et al. 2015), which may be enhanced by local pollution (Baker et al. 2010). In the case of octocorals, the importance of autotrophy and heterotrophy and their respective contributions to the host's energy budget are scarcely studied (but see Ribes et al. 1998; Pupier et al. 2019), though it might be one of the key elements for understanding their successful distribution in the new reef panorama, created by disturbance-induced transitions from scleractinian-to-octocoral-dominated seascapes (reviewed in Schubert et al. 2017). Such transformations result in changes in ecosystem functioning and loss of ecosystem services (Hughes et al. 2017). Thus, the knowledge of autotrophic and heterotrophic energy contributions in mixotrophic octocorals and their flexibility under environmental changes will advance our understanding about their importance in the benthic–pelagic coupling and the oceanic carbon cycle (see Coppari et al. 2019). This information will also help explain octocorals prevalence over scleractinian corals in different areas of the Caribbean (and also in other tropical areas; reviewed in Schubert et al. 2017).

In this context, studying the seasonal trends of autotrophic and heterotrophic inputs represents an essential yet understudied approach. Until now, studies have focused solely on one of these energy strategies (Fabricius and Klumpp 1995; Ribes et al. 1998; Baker et al. 2015; Pupier

et al. 2019) and their seasonal variation (Bednarz et al. 2015; Coma et al. 2015). The latter has been well studied for the heterotrophic energy input in warm-temperate non-symbiotic octocorals, in order to understand reproductive cycles, energy investment in respiration, trophic crises, and population dynamics under the seasonal availability of food (Ribes et al. 1999; Rossi et al. 2004; Tsounis et al. 2006, 2010; Coma et al. 2015; Rossi et al. 2017b and references therein), and hence, potential deficits or surpluses in energy input (Coma et al. 1998; Coppari et al. 2016). Yet, to our knowledge, only Farrant et al. (1987) studied both the seasonal variation in autotrophic and heterotrophic inputs in the temperate octocoral *Capnella gaboensis*.

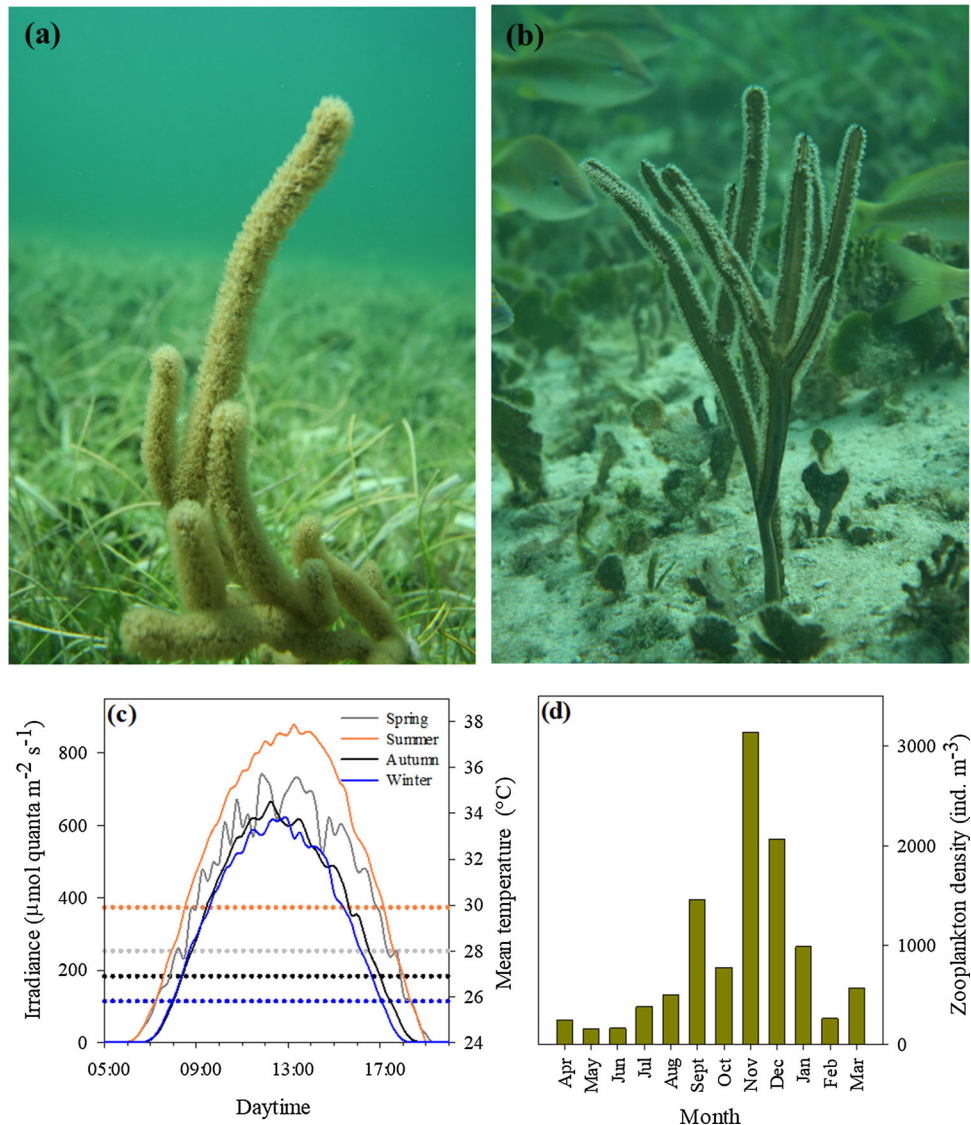
In this study, we used an integrated approach to determine heterotrophic and autotrophic contributions to the hosts' energy demand in the representative Caribbean octocorals *Pterogorgia anceps* and *Plexaurella nutans* (Jordán Dahlgren 1989), as well as potential seasonal variations in these contributions. To achieve these objectives, we (1) quantified the monthly zooplankton capture rates (polyp gut contents), (2) analyzed monthly variation in tissue carbon and nitrogen and $\delta^{13}\text{C}$ and $\delta^{15}\text{N}$ stable isotope contents to understand the trophic position of both species throughout the year, (3) quantified the monthly variation in Symbiodiniaceae (of the genus *Breviolum*) cell density and pigment content, and (4) performed seasonal measurements of algal symbiont photosynthetic performance and host respiratory demand. Furthermore, based on the data and information about colony density and population structure of the gorgonians in the studied tropical reef lagoon, we estimated the impact of the two gorgonians in the carbon cycle and benthic–pelagic coupling processes.

Materials and methods

Sampling site and collection

Between April 2014 and April 2015, samples from two octocoral species, *Pterogorgia anceps* (Pallas 1766) and *Plexaurella nutans* (Duchassaing and Michelotti 1860) (Fig. 1a, b), were collected monthly in the same area at ~ 2 m depth in the Puerto Morelos reef lagoon, Mexican Caribbean ($20^{\circ} 50' 57.8659''$ N, $86^{\circ} 52' 34.6967''$ W). The lagoon experiences seasonal variations in temperature (mean temperature range 25–30 °C) and light (max. daily intensity range 200–1800 $\mu\text{mol quanta m}^{-2} \text{s}^{-1}$), data that were obtained from the Oceanographic and Meteorological Academic Service (SAMMO) of the UNAM Coral Reef Systems Academic Unit in Puerto Morelos. The monthly variation in light level at collection depth was calculated,

Fig. 1 Octocorals **a** *Plexaurella nutans* and **b** *Pterogorgia anceps* in the Mexican Caribbean reef lagoon of Puerto Morelos. Seasonal variation (2014/2015) in **c** the light environment at 2 m collection depth (67% incident light, $K_d = 0.2 \text{ m}^{-1}$), with the respective mean temperature (dotted lines) and **d** the monthly variation in zooplankton density in the reef lagoon (from Álvarez-Cadena et al., 2009). Incident light was recorded by the Oceanographic and Meteorological Academic Service (SAMMO) of the UNAM Coral Reef Systems Academic Unit in Puerto Morelos



using the reported light attenuation coefficient for the lagoon ($K_d = 0.2 \text{ m}^{-1}$; Enríquez and Pantoja-Reyes 2005), showing light levels of 67% of incident light at 2 m depth and a variation in mean seasonal maximum light intensity between 620 and 880 $\mu\text{mol quanta m}^{-2} \text{ s}^{-1}$ (Fig. 1c). In addition to abiotic parameters, also a strong seasonal pattern in zooplankton density in the Puerto Morelos reef lagoon had been reported previously, with recorded higher abundances during summer/autumn (Fig. 1d; Álvarez-Cadena et al. 2009).

During the monthly sampling, branches of ten different colonies (5–8 cm height; $n = 1$ per colony) of each of the two species were collected and afterward taken immediately to the laboratory, where they were divided into two subsamples. The apical part was frozen at $-80 \text{ }^\circ\text{C}$ for subsequent analyses of organic matter content, stable isotopes, and algal symbiont densities and pigment contents,

and the basal part was fixed in 6% formalin for gut content analysis. Before freezing, photographs of the samples were taken (putting a ruler next to the sample) for later surface area determination. In addition, once per season (May, July, October, and January), branches from five colonies per species were collected for physiological measurements. After sampling, they were fixed with non-toxic rubber and maintained in seawater flow-through tanks for a day under ambient light, adjusted to the levels at collection depth, to allow recovery from handling, before the incubations for photosynthesis and respiration determinations.

Colony morphology

To characterize colony morphology and any potential differences between species that subsequently might affect their feeding efficiency, photographs were taken from

different colonies of *P. anceps* ($n = 43$) and *P. nutans* ($n = 58$). From those, colony size and number of branches per order and their respective length and width were determined. Subsequently, the total area (in cm^2) was calculated from these measurements, to determine the mean number of polyps per colony, using polyp densities of the species as reported in Rossi et al. (2018), and the heterotrophic carbon uptake of the species per m^2 seafloor.

Gut contents and prey carbon determination

Feeding on zooplankton was assessed by means of gut content examinations of apical fragments, using a total of 100 polyps per monthly sample ($n = 10$ branches and $n = 10$ polyps per branch) and species, selected at random. The polyps were isolated by dissection under a binocular microscope, and the gut contents were identified to the highest taxon level and counted. The zooplankton capture rate (ZC) expressed as the number of prey items captured per polyp and per hour was calculated using the following equation (Coma et al. 1994):

$$\text{ZC} (\text{prey polyp}^{-1} \text{h}^{-1}) = N [\Sigma(1 - t/D)]^{-1} \quad (1)$$

where N is the number of prey items per polyp, t is the time (1 h), and D is the digestion time (in hours). Unfortunately, prey digestion times are not available for the studied species. Thus, and considering the variation with temperature, reported values for other sessile cnidarian species and different temperatures were used to obtain a relationship between temperature and digestion time (Fig. S1, Table S1). The obtained digestion time, used to calculate ZC, varied between one to four hours, when considering the monthly temperature variation.

Based on Eq. (1), also carbon ingestion rates were calculated, using instead of the number of prey items per polyp, the corresponding carbon ingested per polyp (in μg). These data were obtained by measuring the size of the prey under the microscope, estimating prey biomass from biovolume (Sebens and Koehl 1984) and using conversion factors for wet weight (Hall et al. 1970), dry weight (13% of wet weight; Beers 1966), and carbon content (45% of dry weight; Biswas and Biswas 1979).

Organic matter

The organic matter (OM) content was determined by subsampling 300–500 mg of the coenenchyma of the freeze-dried tissue ($n = 10$ per species and month). Samples were combusted in a muffle furnace (Relp 2H-M9) at 500 °C for 4 h, and the remaining inorganic ash was weighed. The OM content (ash-free dry weight, AFDW) was calculated from the difference between dry weight (DW) and ash

weight (AW) (Slattery and McClintock 1995; Rossi et al. 2006).

Tissue carbon and nitrogen content and stable isotopes

Three replicates of freeze-dried branches were analyzed per species and month. The material (0.50–1.1 mg) was slightly acidified with 10% hydrochloric acid (HCl), in order to remove carbonates, which can bias $\delta^{13}\text{C}$ signatures (Jacob et al. 2005), following protocols of McConnaughey and McRoy (1979), Hobson and Welch (1992), and Jacob et al. (2005).

The $\delta^{13}\text{C}$ and $\delta^{15}\text{N}$ stable isotope analyses were performed with a mass spectrometer (Flash EA 1112 HT O/H-N/C), following the same procedure as previously described in Elias-Piera et al. (2013). Isotopic ratios were expressed as parts per thousand (‰) (difference from a standard reference material) in accordance with the following equation:

$$\delta X = [(R_{\text{sample}}/R_{\text{standard}}) - 1] \times 10^3 \quad (2)$$

where X is either ^{13}C or ^{15}N and R is the corresponding ratio ($^{13}\text{C}/^{12}\text{C}$ or $^{15}\text{N}/^{14}\text{N}$). Standard R values for ^{13}C and ^{15}N were from PeeDee Belemnite (PDB) and atmospheric N_2 , respectively.

Determination of Symbiodiniaceae cell density and chlorophyll content

Algal symbiont cell densities and chlorophyll (Chl a and c_2) concentrations were determined ($n = 10$ per species and month) by adding filtered seawater to the tissue samples to a final volume of 5 mL and homogenizing them with a tissue homogenizer (IKA Ultra-Turrax, Sigma-Aldrich). Afterward, the samples were centrifuged at $1500\times g$ for 15 min, the supernatant discarded and the pellet resuspended in 5 mL filtered seawater, and subsamples were taken for subsequent cell density and chlorophyll determinations. A subsample of 1 mL was taken from the resuspended tissue pellet, fixed with Lugol's solution, and subsequently, the symbiont cells were counted using an improved Neubauer hemocytometer and normalized to ash-free dry weight and surface area. To determine chlorophyll concentrations, the pigment extraction was performed as outlined by Iglesias-Prieto et al. (1992) and chlorophyll a (Chl a) and c (Chl c_2) contents were calculated using the equations of Jeffrey and Humphrey (1975). Chlorophyll concentrations were normalized to ash-free dry weight, surface area, and symbiont cell density.

Photosynthetic performance

To determine oxygen fluxes of the octocorals, branches ($n = 5$ per species and season) were incubated in a sealed temperature-controlled acrylic dual chamber at the temperature in the reef lagoon measured during sampling (see Rossi et al. 2018 for details). The incubations were performed by exposing the samples to increasing light intensities, with dark incubations at the beginning and the end of the exposures to determine dark (R_D) and light respiration rates (R_L). The changes in oxygen concentration were recorded, using an optode system, connected to a computer running the Pyro Oxygen Logger (FireSting Pyroscience, Aachen, Germany). The photosynthetic parameters were normalized by ash-free dry weight or surface area, and the gross photosynthetic rates were calculated by adding respiration (average between R_D and R_L) to net photosynthesis. The highest photosynthetic rate was considered as P_{max} , and the photosynthetic efficiency (α) was estimated from the initial slope of the light-response curve by linear least-square regression analysis.

Autotrophic and heterotrophic carbon budgets

Daily host carbon metabolic demand (respiratory carbon loss— R_c) and gross autotrophic carbon assimilation (GP_c) were calculated from daily gross photosynthetic and respiration rates, obtained by integrating the seasonal P–I curves against the respective daily variation in the mean monthly irradiance at collection depth (see Rossi et al. 2018). The latter was calculated from incident light data and a light attenuation coefficient (K_d) of 0.2 m^{-1} (see Enríquez and Pantoja-Reyes 2005). For daily integration of respiration, the determined rates in dark (R_D) and light (R_L), in combination with the light to dark hours of the respective season, were used. Afterward, the daily integrated gross photosynthesis (GP) and respiration (R; in $\mu\text{mol O}_2 \text{ g}^{-1} \text{ AFDW day}^{-1}$) were converted into carbon equivalents, based on molecular weights and using the photosynthetic (PQ) and respiratory quotients (RQ), according to Muscatine et al. (1981):

$$GP_c = \text{mg O}_2 \text{ produced} \cdot 0.375 \text{ PQ}^{-1} \quad (3)$$

$$R_c = \text{mg O}_2 \text{ consumed} \cdot 0.375 \text{ RQ} \quad (4)$$

where PQ and RQ are assumed to be 1.1 and 0.8, respectively.

The heterotrophic carbon input was estimated by extrapolating the zooplankton capture rate over a 24-h cycle, and the obtained daily heterotrophic carbon input through prey capture and ingestion (H_c) was then used to calculate the seasonal variation in CHAR (% contribution of heterotrophically acquired carbon alone to meet daily

carbon demand) according to Grottoli et al. (2006), assuming that all of the carbon in zooplankton is biologically available:

$$\text{CHAR} = H_c/R_c \times 100\% \quad (5)$$

In addition, based on the estimated daily R_c and GP_c and heterotrophic carbon input (H_c), the scope for growth plus excretory losses (SfG'), which defines the amount of carbon (acquired autotrophically and heterotrophically) that is available to an organism for growth and reproduction, after maintenance costs have been accounted for, was calculated as in Anthony and Fabricius (2000):

$$SfG' = GP_c + H_c - R_c \quad (6)$$

Statistical analyses

The assumptions of normality and homoscedasticity were tested using the Shapiro–Wilk's and the Levene tests, respectively. In the case of host parameters (prey per polyp, prey size, prey ingestion, AFDW, H_c , stable isotope data) and Symbiodiniaceae parameters (cell density, chlorophyll concentration, C_i) throughout the year, the homoscedasticity assumption was satisfied, but not normality. Thus, they were analyzed using the nonparametric Kruskal–Wallis test. However, for the photosynthetic parameters, parametric analyses of variance (two-way ANOVA) and Newman–Keuls post hoc tests allowed for the determination of significant differences ($p < 0.05$) between seasons and species. The statistical analyses were conducted using Statistica 12.0.

Results

Colony morphology

The biometry of the two studied species, *Pterogorgia anceps* and *Plexaurella nutans*, was not significantly different, with colony heights of 33 ± 9 and 36 ± 11 cm, respectively. Both species exhibited similar numbers and length of branches per order (Table 1) and based on polyp densities reported for the two species, *P. anceps* and *P. nutans* exhibit mean values of 2330 and 2028 polyps colony⁻¹, respectively.

Annual variation in heterotrophic feeding and organic biomass

The size of prey found within the octocoral polyps did not differ significantly among species ($H = 3.79$, $p = 0.0515$), but varied seasonally in *P. anceps* ($H = 8.37$, $p = 0.0390$). Here, larger prey was found during spring and summer

Table 1 Colony morphology. Comparison of number of branches and lengths between *Pterogorgia anceps* ($n = 43$) and *Plexaurella nutans* ($n = 58$) and summary of Kruskal–Wallis tests for differences between species

Order	Number of branches		Mean branch length (cm)	
	<i>P. anceps</i>	<i>P. nutans</i>	<i>P. anceps</i>	<i>P. nutans</i>
First	13.3 ± 0.9	11.1 ± 0.6	12.8 ± 0.7	18.6 ± 1.1
Second	4.3 ± 0.4	3.8 ± 0.2	6.5 ± 0.4	6.5 ± 0.3
Third	2.4 ± 0.3	1.6 ± 0.2	5.9 ± 0.3	4.9 ± 0.2
Kruskal–Wallis species	$H = 3.183, p = 0.0744$		$H = 0.0386, p = 0.8443$	

Data are shown as mean ± SE

months (Fig. 2a), composed mainly of copepods, Cirripedia larvae, and organic matter particles (Table S2). In contrast, no seasonal differences were found in *P. nutans* ($H = 0.235, p = 0.9717$), with prey sizes similar to the ones found in *P. anceps* during autumn and winter (mostly copepods, nauplii and eggs; Table S2).

Generally, both species exhibited higher capture rates during late summer, though the determined prey capture was significantly different between species (Table 2). This was related to two strong peaks in *P. anceps* in September and November, surpassing zooplankton capture of *P. nutans* by a factor of 7 and 9.5, respectively (Fig. 2b).

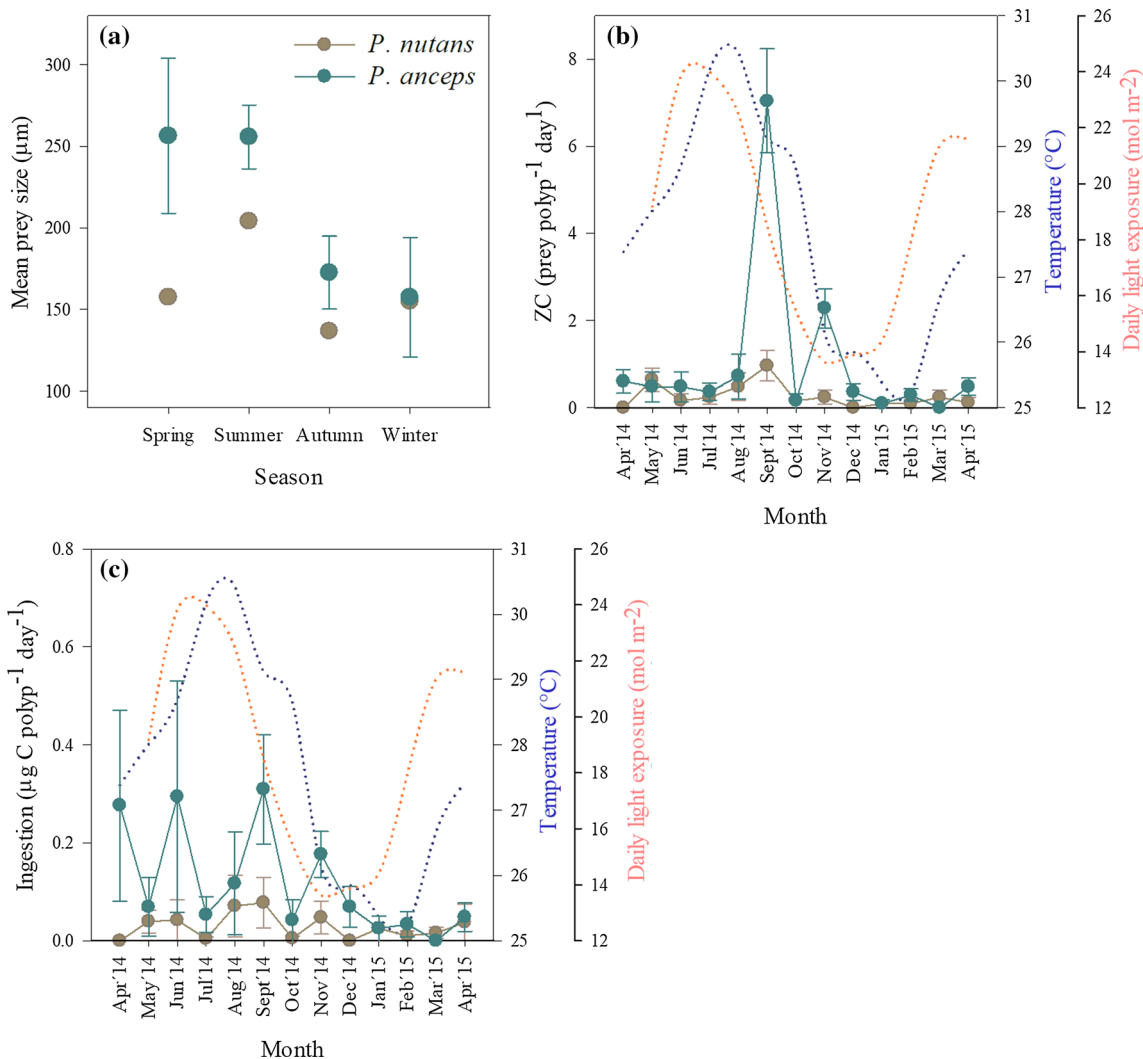


Fig. 2 Heterotrophic feeding of two Caribbean octocorals. **a** Seasonal variation in mean prey size, **b** monthly variation of prey capture (considering a 24-h cycle of polyp activity), and **c** the corresponding heterotrophic carbon ingestion rate of *P. nutans* and *P. anceps* over an

annual cycle. Data represent mean ± SE ($n = 10$ per month and species), and annual variation in seawater temperature (blue) and irradiance at collection depth (orange) are indicated by dotted lines

Table 2 Summary of Kruskal–Wallis tests for the differences in host—(zooplankton capture rate—ZC, heterotrophic carbon ingestion, tissue carbon and nitrogen content, stable isotopes), and symbiont-related parameters (symbiont cell density and pigment content) of *Plexaurella nutans* and *Pterogorgia anceps* between species and sampling months ($p < 0.05$ is indicated in bold)

Parameter	Species		<i>P. nutans</i> -Month		<i>P. anceps</i> -Month	
	<i>H</i>	<i>p</i>	<i>H</i>	<i>P</i>	<i>H</i>	<i>p</i>
Host						
ZC (prey polyp ⁻¹ day ⁻¹)	9.20	0.0024	19.3	0.0553	64.2	< 0.00001
Ingestion (μg C polyp ⁻¹ day ⁻¹)	9.95	0.0016	9.13	0.6092	35.2	0.0002
Tissue carbon (%)	49.4	< 0.00001	12.5	0.3298	14.9	0.1832
Tissue nitrogen (%)	43.8	< 0.00001	12.3	0.3440	18.2	0.0768
δ ¹³ C (‰)	35.9	< 0.00001	12.9	0.3030	16.9	0.1105
δ ¹⁵ N (‰)	31.1	< 0.00001	12.3	0.3406	21.8	0.0258
AFDW (g cm ⁻²)	103.4	< 0.00001	42.7	< 0.00001	75.9	< 0.00001
Symbionts						
Cell density (g ⁻¹ AFDW)	3.28	0.0703	44.2	< 0.00001	52.6	< 0.00001
Chlorophyll <i>a</i> + <i>c</i> (g ⁻¹ AFDW)	4.57	0.0325	44.0	< 0.00001	54.8	< 0.00001
<i>C_i</i> (μg Chl <i>a</i> + <i>c</i> cell ⁻¹)	19.3	< 0.00001	67.3	< 0.00001	34.0	0.0004

Together, larger prey size and the observed peaks in prey capture led to significantly higher and seasonally varying heterotrophic carbon ingestion of *P. anceps* (annual mean ± SD: 0.12 ± 0.11 μg C polyp⁻¹ day⁻¹), with the lowest values found during winter (Fig. 2c; Table 2). On the other hand, the heterotrophic ingestion in *P. nutans* was significantly lower and varied little during the year (0.03 ± 0.03 μg C polyp⁻¹ day⁻¹) (Fig. 2c; Table 2).

The organic biomass per surface area varied significantly over the year and also between months in both species (Table 2). Generally, the lowest values were found during summer and in December, while the highest values were recorded during spring and winter, with a peak in October and November in *P. nutans* and *P. anceps*, respectively (Fig. S2).

Annual variation in tissue carbon and nitrogen content and stable isotopes

The carbon tissue content differed significantly among species, with an annual mean value of 7.0 ± 1.1% in *P. nutans* and 1.51 ± 2.7% in *P. anceps* (Fig. 3a). In the latter species, sampling months did not affect carbon contents (Table 2). A similar pattern was found for the tissue nitrogen content, again with significantly higher values in *P. anceps* (annual mean ± SD: 2.8 ± 0.6%), than in *P. nutans* (1.5 ± 0.2%) (Fig. 3b; Table 2).

As with the tissue carbon and nitrogen contents, the stable isotope analyses revealed significant differences between the two species (Table 2). Here, *P. anceps* exhibited mean annual δ¹³C values of -15.6‰ and *P. nutans* of -16.5‰, while mean δ¹⁵N values of 4.2 and 5.2‰ were found in *P. nutans* and *P. anceps*, respectively (Fig. 3c, d). Also, in *P. anceps*, the sampling month exerted a significant effect on the δ¹⁵N values (Table 2).

Annual variation in Symbiodiniaceae density and pigment content

In both octocoral species, symbiont parameters varied significantly depending on the sampling month, with species-specific differences in pigment content per AFDW and per symbiont cell, though not in the number of symbiont cells per AFDW (Table 2). The mean annual symbiont cell density in both species was 138–147 × 10⁶ cells g⁻¹ AFDW, which exhibited a peak in December, increasing by a factor of two and four, compared to the previous month, in *P. nutans* and *P. anceps*, respectively (Fig. 4a).

While both species did not differ in their symbiont cell density per AFDW, they did show significant differences in total chlorophyll content per AFDW and, hence, the chlorophyll content per symbiont cell (*C_i*) (Table 2). The mean annual values for total pigment content and *C_i* ranged from 1.0 to 1.2 mg Chl (*a* + *c*) g⁻¹ AFDW and between 6.9 and 8.1 μg Chl (*a* + *c*) cell⁻¹, respectively, with the highest values in both parameters corresponding to *P. anceps*. These parameters also were influenced by season, showing peaks in late summer and late autumn/early winter in the case of *P. anceps*, while *P. nutans* showed a smaller peak in November and a strong increase in late winter (Fig. 4b, c).

The patterns were slightly different when the parameters were normalized by tissue surface area due to the species' differences in biomass per area (Fig. S2). Although they exhibited significant monthly differences, the mean symbiont cell density per cm² was significantly different between the species (mean value of 3.2 and 1.6 × 10⁶ cells cm⁻² in *P. nutans* and *P. anceps*, respectively; Fig. S3a; Table S3). Here, a clearer seasonal pattern was found, with the highest cell density occurring in spring that decreased during summer and subsequently increased again in

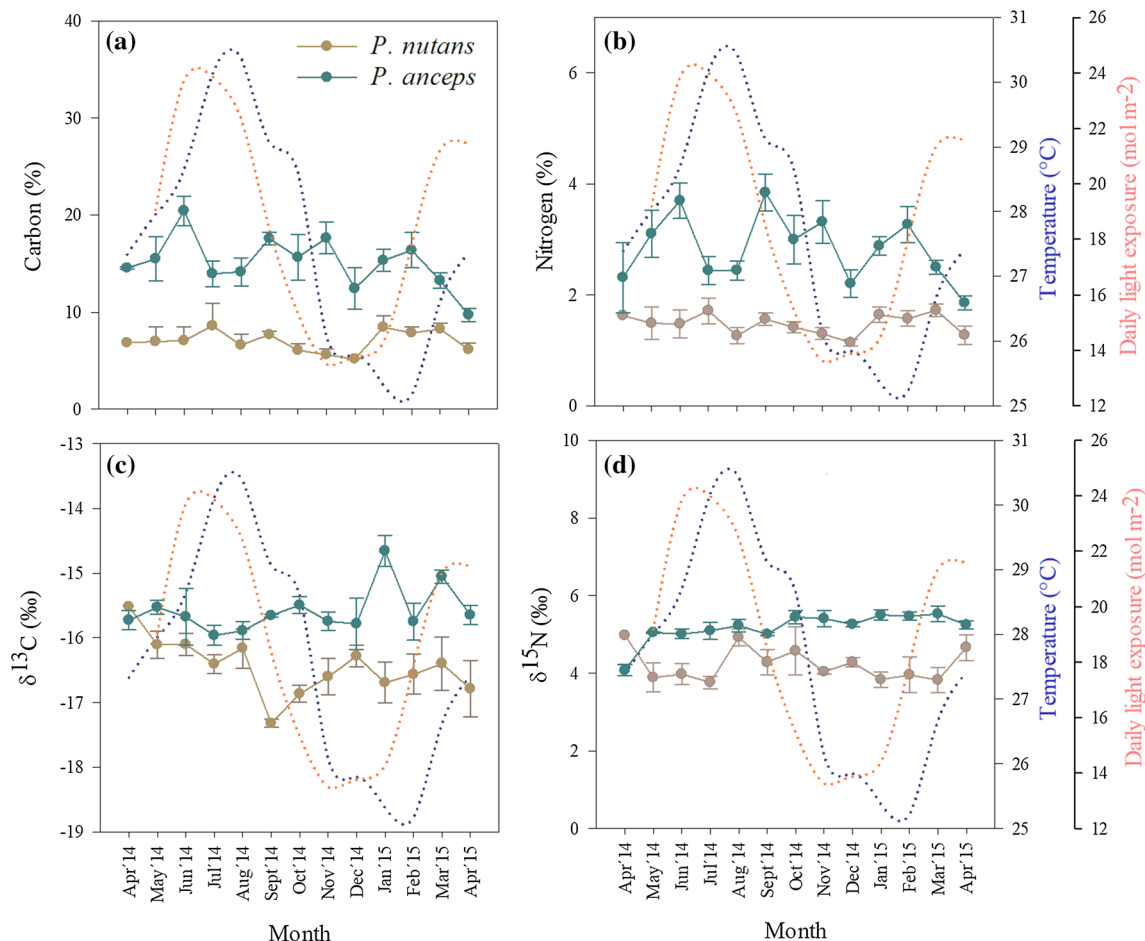


Fig. 3 Stable isotopes in two Caribbean octocorals. Monthly variation in **a** tissue carbon content, **b** tissue nitrogen content, **c** $\delta^{13}\text{C}$ and **(d)** $\delta^{15}\text{N}$ in *P. nutans* and *P. anceps* over an annual cycle. Data

autumn (Fig. S3a). Also, similarly as found for symbiont cell density, when normalized by surface area, *P. nutans* exhibited a higher chlorophyll concentration and a decrease in pigment content during summer, followed by an increase in autumn (Fig. S3b).

Seasonal variation in autotrophic and heterotrophic carbon metabolism

The seasonally performed physiological measurements on the two octocoral species showed significant changes in their photosynthetic performance (Fig. S4) and differences between species when normalized by AFDW, while no differences between the species were found when normalized by surface area (Table S4, S5). The same pattern was found for the daily integrated metabolic rates, gross autotrophic carbon assimilation (GP_c), and respiratory carbon loss (R_c), derived from those measurements (by AFDW; Fig. 5; Table 3), which showed that *P. nutans* achieved the highest values for both GP_c and R_c in spring

represent mean \pm SE ($n = 3$ per month and species), and annual variation in seawater temperature (blue) and irradiance at collection depth (orange) are indicated by dotted lines

and summer, with the lowest rates found in winter (Fig. 5a, c). The latter was also found in *P. anceps*, though this species exhibited higher daily metabolic rates (Fig. 5b, d). The resulting ratios between autotrophic carbon input and respiratory carbon loss (GP_c/R_c) did not show significant differences between the two species, but were influenced by season, with species-specific seasonal responses (Table 3). The GP_c/R_c of *P. nutans* was highest in autumn, reaching a value of 2.1, while similar GP_c/R_c was found during the other seasons, ranging between 1.4 and 1.5 (Fig. 5e). *Pterogorgia anceps*, on the other hand, expressed similar GP_c/R_c of 1.6–1.7 from summer to winter, but with a significantly lower ratio in spring (1.0; Fig. 5f).

As for the daily autotrophic carbon input, the species also differed in the heterotrophically derived carbon intake ($H = 10.92$, $p = 0.0010$), with significantly lower heterotrophic carbon input (H_c) in *P. nutans*, compared to *P. anceps* (Fig. 6). The annual mean for H_c of the former species was $0.024 \text{ mg C g}^{-1} \text{ AFDW day}^{-1}$, while *P. anceps* achieved a rate of $0.173 \text{ mg C g}^{-1} \text{ AFDW day}^{-1}$.

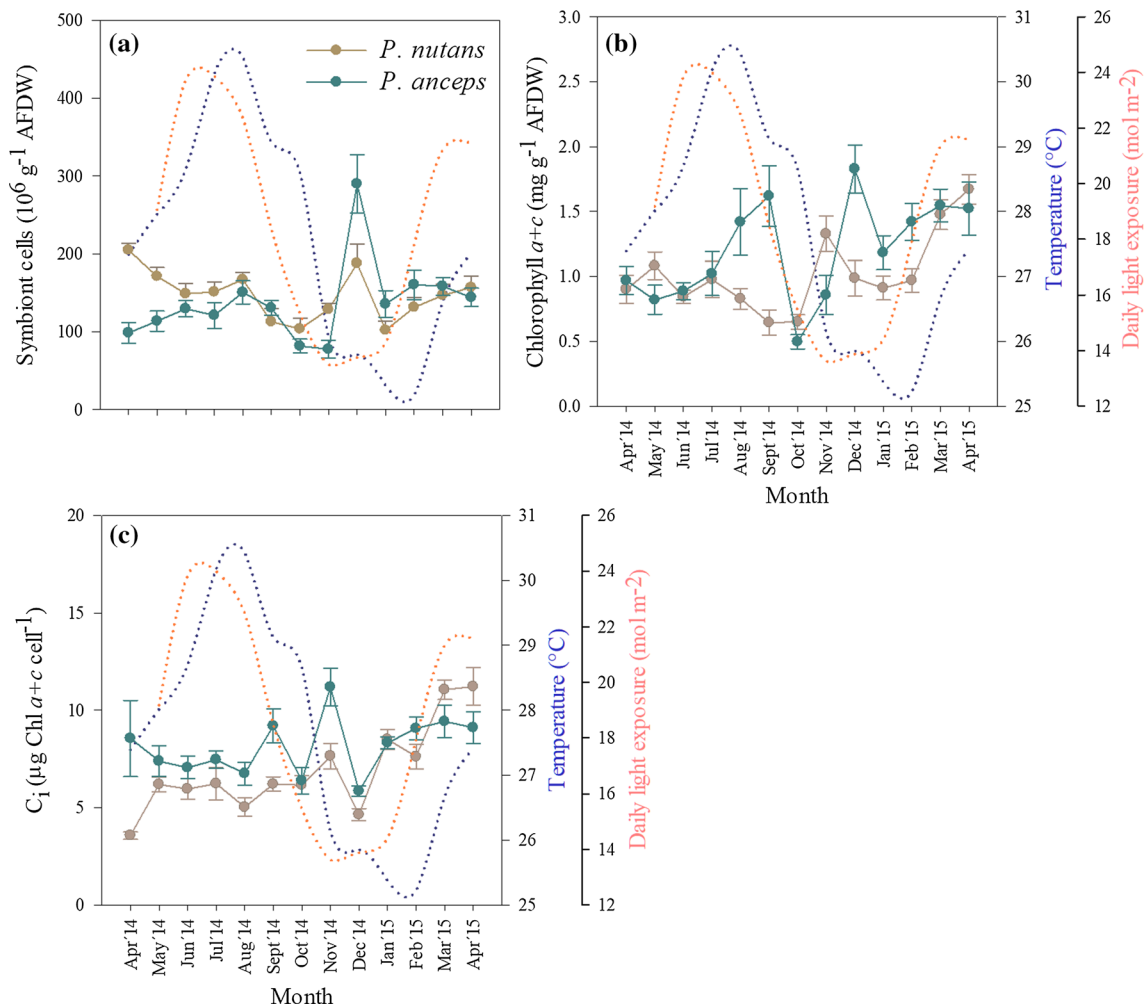


Fig. 4 Symbiodiniaceae (*Breviolum* sp.) density and pigment content in two Caribbean octocorals. **a** Monthly variation in algal symbiont cell density, **b** pigment content, and **c** pigment content per algal symbiont cell of *P. nutans* and *P. anceps* over an annual cycle. Data

represent mean \pm SE ($n = 10$ per month and species), and annual variation in seawater temperature (blue) and irradiance at collection depth (orange) are indicated by dotted lines

Furthermore, *P. nutans* did not show significant seasonal differences in H_c ($H = 0.22$, $p = 0.9739$). In *P. anceps*, though H_c was 4–10 times lower in winter compared to the other seasons, these seasonal differences were also not statistically significant (Fig. 6; $H = 7.13$, $p = 0.0679$). The aforementioned species-specific and seasonal patterns were also reflected in the CHAR (% contribution of heterotrophically acquired carbon to metabolic carbon demand), which was lower in *P. nutans* (0.24–0.80%), compared to *P. anceps* (0.72–3.4%). In the latter, the highest CHAR was estimated in spring and summer, while *P. nutans* exhibited the opposite pattern (Fig. 6).

Considering the estimated daily autotrophic and heterotrophic carbon input, the resulting scope for growth and excretion (SfG') suggested that these octocoral species had a surplus of energy for growth, reproduction, and excretion during most of the year (Fig. 7). An exception, however,

was found in *P. anceps* in spring, where SfG' was almost non-existent, with only $0.04 \text{ mg C g}^{-1} \text{ AFDW day}^{-1}$ (Fig. 7b). Generally, the amount of energy surplus was lower in *P. nutans* (mean: $2.7 \text{ mg C g}^{-1} \text{ AFDW day}^{-1}$), decreasing throughout the year from spring to winter (Fig. 7a). The pattern found in *P. anceps* (mean $3.7 \text{ mg C g}^{-1} \text{ AFDW day}^{-1}$) was different, with the highest SfG' found in summer and autumn (Fig. 7b).

Discussion

This study shows that autotrophic input through the symbiosis with photosynthetic dinoflagellates of the family Symbiodiniaceae represents the main energy source for the demands of the tropical octocoral hosts *Plexaurella nutans* and *Pterogorgia anceps*, supplemented by heterotrophic

Fig. 5 Seasonal variation in **a**, **b** daily metabolic carbon demand (R_c), **c**, **d** daily gross autotrophic carbon assimilation (GP_c), and **d**, **e** their ratio in *P. nutans* and *P. anceps*. Data represent mean \pm SE ($n = 5$ per season and species), and different letters indicate significant differences (ANOVA, Newman–Keuls, $p < 0.05$) between seasons

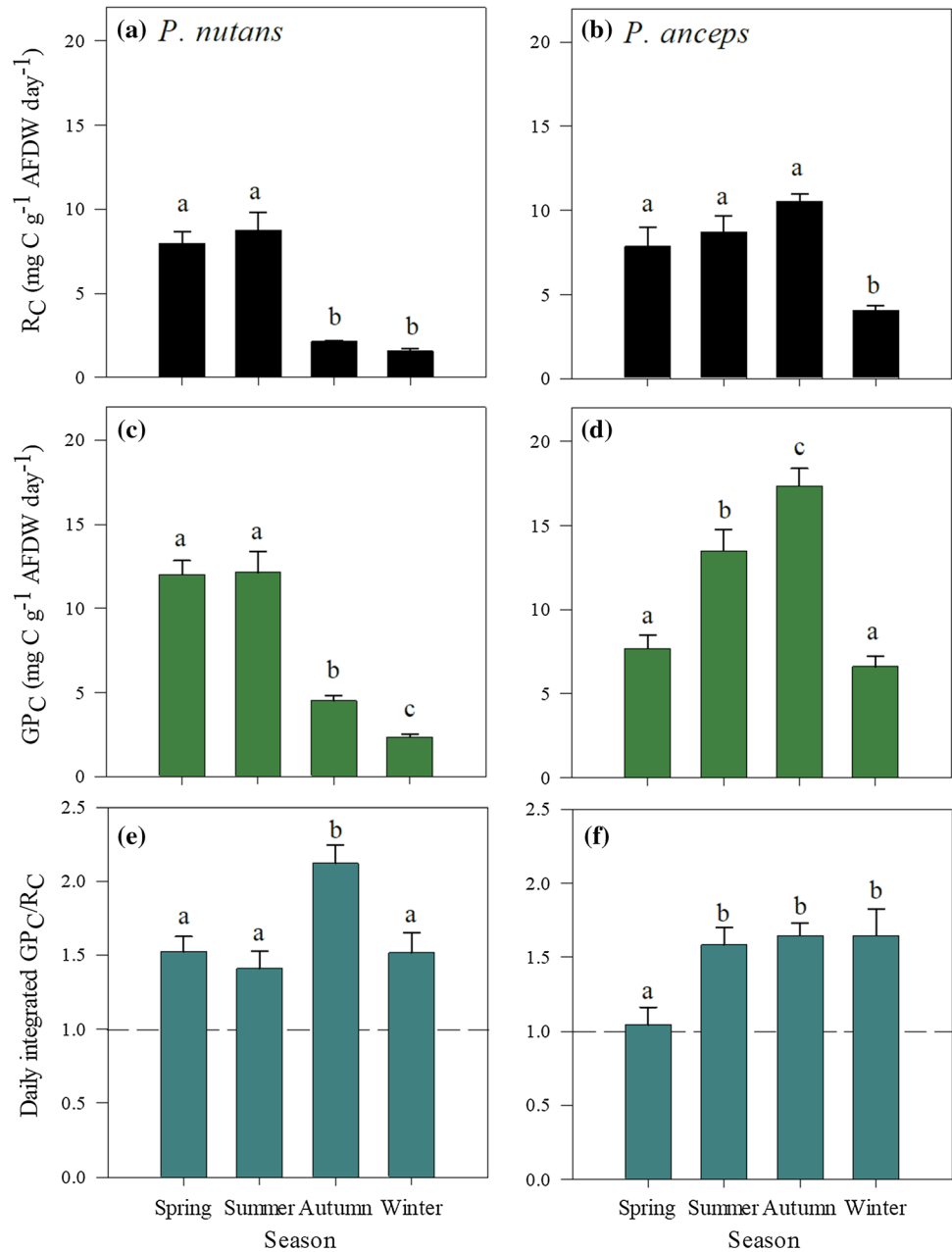


Table 3 Summary of the two-way ANOVA examining for the influence of season and species on daily gross and net autotrophic carbon assimilation (GP_c and NP_c), host respiratory carbon demand (R_c), and the ratio of GP_c/R_c

Parameter	Species		Season		Species x Season	
	<i>F</i>	<i>p</i>	<i>F</i>	<i>p</i>	<i>F</i>	<i>p</i>
GP_c	28.9	< 0.00001	29.9	< 0.00001	29.8	< 0.00001
NP_c	3.15	0.0855	9.71	0.00011	14.5	< 0.00001
R_c	23.8	< 0.00001	22.8	< 0.00001	13.2	< 0.00001
GP_c/R_c	3.85	0.0587	9.17	0.00017	4.85	0.00703

$p < 0.05$ are indicated in bold

Fig. 6 Seasonal variation in the potential daily carbon acquisition from heterotrophy (H_c) in *P. nutans* and *P. anceps*. Data represent mean \pm SE ($n = 30$ per season and species), and numbers indicate the respective CHAR (% contribution of heterotrophically acquired carbon to metabolic carbon demand— R_c)

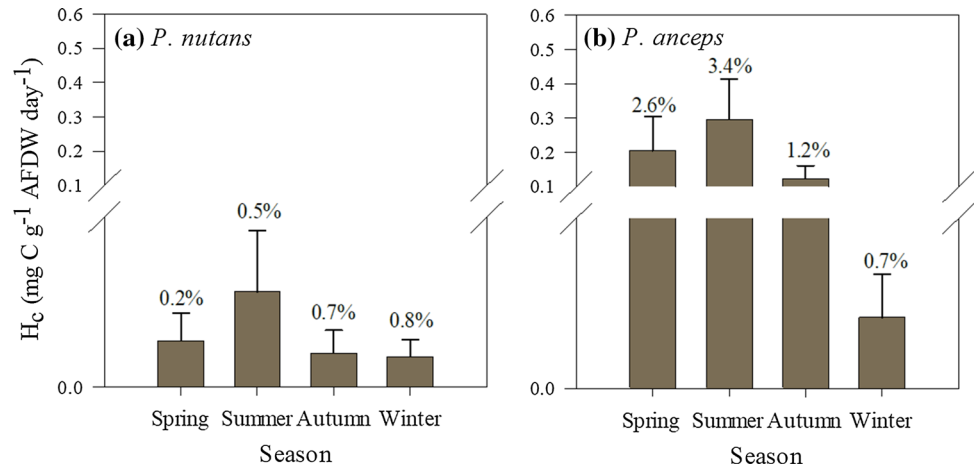
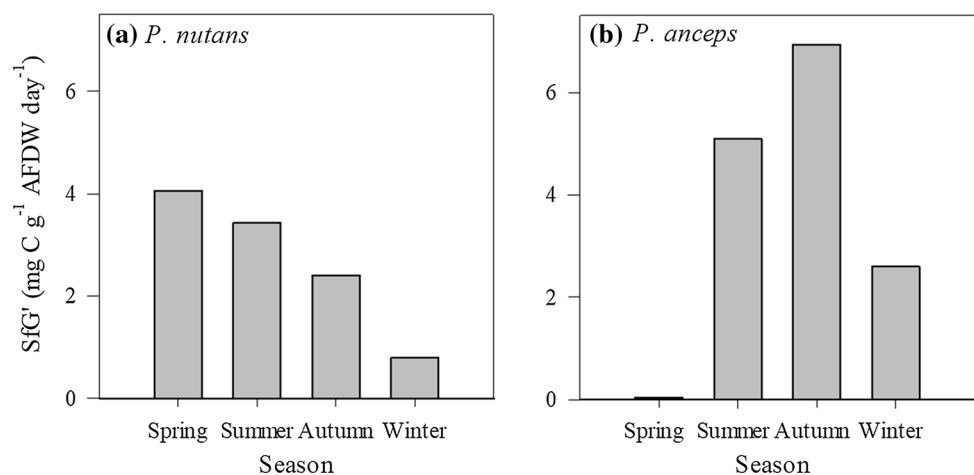


Fig. 7 Amount of organic carbon, acquired through autotrophy and heterotrophy that is potentially available to the octocorals, after accounting for respiratory losses (scope for growth and excretion— SfG' ; Anthony and Fabricius 2000)



zooplankton feeding. It further demonstrates that there exist species-specific and seasonal differences in the contributions of these two nutrition modes, though without indications of shifts in the predominant mode during the year.

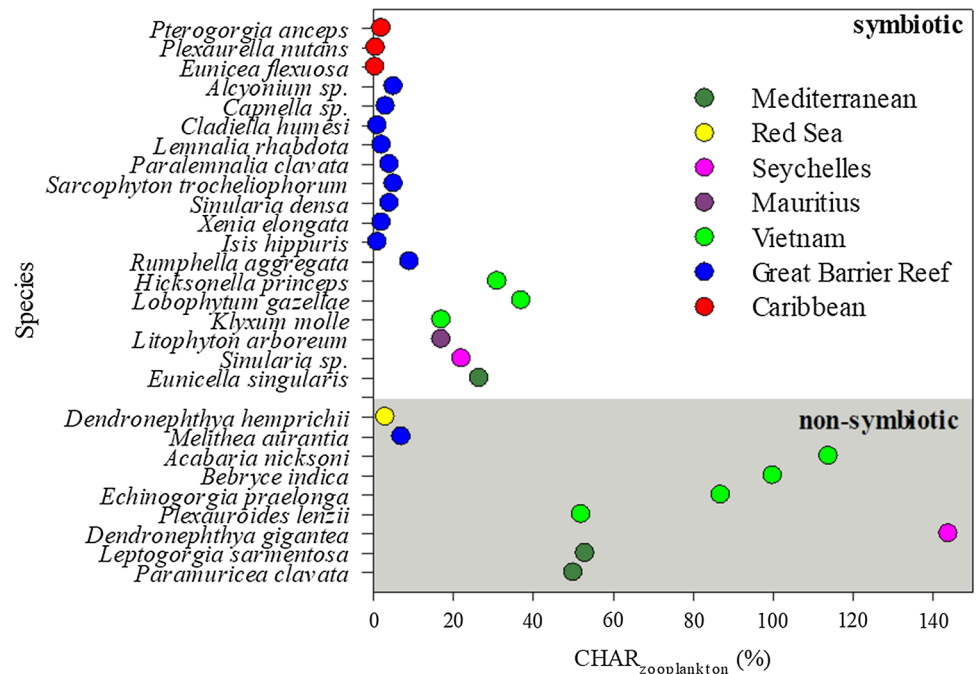
Heterotrophic versus autotrophic carbon input

Heterotrophic energy input through zooplankton feeding was found in both tropical gorgonians, though our data suggest that its contribution to the holobionts' energy demands is low compared to the autotrophic input, as evidenced by the low prey capture rates, CHAR values, and stable isotope signatures.

In general, the gut content analysis showed that crustaceans were the main prey found in both species (Table S2), which was not surprising, as they dominate the zooplankton in the Puerto Morelos lagoon (Álvarez-Cadena et al. 2009). Though studies on heterotrophic prey capture and carbon input in Caribbean symbiotic octocorals are scarce, the prey size found here (60–580 μm) was in line with another study on the Caribbean octocorals

Eunicea flexuosa and *Pseudoplexaura porosa* (100–700 μm ; Ribes et al. 1998). These species also exhibited similar prey capture rates as *P. anceps* and *P. nutans*, which compared to non-symbiotic octocorals, were up to one order of magnitude lower (Table S6). This difference is also reflected in the generally lower CHAR values in symbiotic octocorals, ranging between 0.4 and 37%, compared to 2.4–144% in non-symbiotic species (Fig. 8). In comparison with other tropical- and warm-temperate species, CHAR values determined here for *P. anceps* and *P. nutans* were in the lower range (0.54–1.98%; Fig. 8), supporting our conclusion of a low contribution of heterotrophic feeding to symbiotic octocoral metabolic demands. However, we should point out that only zooplankton feeding was considered here, but phytoplankton, bacteria, and DOM can also account for a high proportion of heterotrophic carbon input in octocorals that can be as high or higher compared to zooplankton feeding (see Table S6). Yet, based on the available information in the Caribbean *Eunicea flexuosa*, where a similar CHAR has been found as in the studied species, phytoplankton seems to account for only a small proportion (CHAR =

Fig. 8 Comparison of reported contribution of heterotrophically acquired carbon from zooplankton to metabolic demands (CHAR) in symbiotic and non-symbiotic octocorals from different regions (for details, see Table S6)



0.4%, of which zooplankton accounted for 0.3%; Ribes et al. 1998). Detritus (in the form of small pieces of macroalgae or seagrasses, dead zooplankton or microphytoplankton mucilage, for example) may be also an important part of the diet of gorgonians (Ribes et al. 1999), but the approach used here cannot quantify this input properly.

Despite the aforementioned limitation, our data showed clearly that in the studied species, autotrophic nutrition had a greater importance, which agrees with other studies on tropical octocorals (Schlichter et al. 1983; Fabricius and Klumpp 1995; Baker et al. 2015). Our conclusion is also supported by the $\delta^{13}\text{C}$ signatures of the species that suggest a mainly autotrophic carbon input. The $\delta^{13}\text{C}$ values of the two studied species (-16.5 and -15.6‰) were in the same range (-18.0 to -11.7‰) as reported in other symbiotic Caribbean octocorals (Table S7; Ward-Paige et al. 2005; Baker et al. 2010, 2015; Crandall 2014; Rossi et al. 2018; Kupfner Johnson 2019; McCauley and Goulet 2019) and symbiotic scleractinian corals (e.g., Muscatine et al. 1989; Nahon et al. 2013), but higher than reported in non-symbiotic Mediterranean octocorals and scleractinian corals (-18 to -24‰ ; Muscatine et al. 1989; Cocito et al. 2013; Leal et al. 2014). The higher $\delta^{13}\text{C}$ signatures of the octocoral tissue, relative to zooplankton and phytoplankton in the Caribbean (-20 to -22‰ ; e.g., Fry and Sherr 1989; Land et al. 2000), indicate that *P. anceps* and *P. nutans* were relying mainly on autotrophy to cover their metabolic demands (most of the carbon came from the photosynthetic activity of Symbiodiniaceae originated through the C4 cycle). This was also supported by the photosynthetic rates of the two species (2.4–12.1 and

6.6–17.4 mg C g^{-1} AFDW day^{-1} for *P. nutans* and *P. anceps*, respectively) that were as high as or mostly higher than the respiratory demand, resulting in GP_c/R_c ratios of 1.0–2.12. Similar autotrophic carbon inputs (4–15.6 mg C g^{-1} AFDW day^{-1}) have also been found in other shallow Caribbean and Indo-Pacific octocoral species (Fabricius and Klumpp 1995; Rossi et al. 2018). Likewise, the here obtained GP_c/R_c and oxygen-based GP/R ratios agree with recently reported ratios in Red Sea octocorals (1–2; Pupier et al. 2019) and those reported in other shallow Caribbean and Indo-Pacific species (Fabricius and Klumpp 1995; Ramsby et al. 2014; Baker et al. 2015; Rossi et al. 2018), respectively.

The significantly higher mean $\delta^{13}\text{C}$ values found in *P. anceps* (-15.6‰) compared to *P. nutans* (-16.5‰) agreed with the higher mean autotrophic input of *P. anceps* (11.3 ± 2.5 mg C g^{-1} AFDW day^{-1} , compared to 7.8 ± 2.5 in *P. nutans*), with not significantly different cell density per AFDW between the two species (Table 2). This was most likely related to the differences in organic biomass per surface area of epidermal tissue of the species (Fig. S2). As this feature determines both gas exchange and light exposure of the Symbiodiniaceae, the almost 2× higher biomass per surface area of *P. nutans* (0.023 ± 0.001 g AFDW cm^{-2}) compared to *P. anceps* (0.012 ± 0.001 g AFDW cm^{-2}) might explain the lower metabolic rates of the former species.

In addition to the evidence provided by the $\delta^{13}\text{C}$ signature of the species, the lower $\delta^{15}\text{N}$ values in *P. anceps* and *P. nutans*, relative to the signatures of particulated organic matter, phytoplankton, and zooplankton (6–7‰,

Land et al. 2000; 3–13‰, Owens 1988), could suggest low heterotrophic contribution, though the interpretation of this signature in symbiotic organisms is difficult as it is affected by different processes. The final signature of the coral tissue represents a mix of different nitrogen sources, due to internal recycling between symbionts and the host, the preferential uptake of ^{14}N by the symbionts, and the assimilation of nitrogen sources with different $\delta^{15}\text{N}$ values (reviewed in Ferrier-Pagès and Leal 2019). This might be responsible for the species-specific variations in $\delta^{15}\text{N}$ values in Caribbean octocorals, ranging between -0.4 and 7.5‰ (Table S7) that are, however, generally lower than the values reported in non-symbiotic Mediterranean octocorals (5–10‰; Cocito et al. 2013; Leal et al. 2014). Despite the aforementioned problems with the interpretation of the $\delta^{15}\text{N}$ regarding heterotrophic input, the significantly higher annual mean $\delta^{15}\text{N}$ values of *P. anceps* (5.2‰), compared to *P. nutans* (4.2‰), together with the gut content analysis, showing that zooplankton feeding was significantly higher in the former species, seem to indicate a higher heterotrophic carbon input in the former species, which also resulted in a higher proportion of CHAR (Fig. 6).

Seasonal variation in heterotrophic and autotrophic inputs

Both species showed seasonal variability in the autotrophic carbon input, but no temporal changes in the heterotrophic contributions to the energy budget. However, similar as in a temperate symbiotic octocoral and tropical scleractinian corals (Nahon et al. 2013; Ferrier-Pagès et al. 2015), no significant seasonal variation in the importance of the two nutrition modes (i.e., trophic shift) was found in either species.

The daily heterotrophic carbon uptake showed a similar seasonal pattern in the two studied species, even though it was generally much lower in *P. nutans*. However, the species differed in the heterotrophic contribution to the host's energy demand, due to differences in seasonal variability in respiratory demand. This resulted in zooplankton ingesta accounting for 2.6–3.4% of the respiratory demand in spring and summer in *P. anceps*, with the lowest contribution found in winter (0.7%), while *P. nutans* showed the lowest contribution in spring (Fig. 6). In this context, no apparent relationship between zooplankton capture rate and the reported seasonal variation in food availability, with highest abundances in late autumn, was found (Fig. 1d; Álvarez-Cadena et al. 2009).

The contribution of the autotrophic energy input to the host's metabolic demands also showed a species-specific pattern, with the highest input found in *P. nutans* in autumn, while *P. anceps* exhibited similar inputs from summer to winter, but much lower values in spring

(Fig. 5e, f). Such seasonal variations have been reported previously, and they seem to differ depending on region and/or species. For example, the lowest autotrophic contributions in the subtropical species *Sarcophyton* spp. were found in summer (Bednarz et al. 2015), while in the temperate species *Capnella gaboensis*, it was highest during summer (Farrant et al. 1987). Also, the mismatch between symbiont photosynthetic performance and the autotrophic energy contribution (Fig. 5c–f) suggests that the seasonal variation in host's respiratory demands (Fig. 5a, b), rather than in symbiont photosynthetic performance, determined the importance of the latter.

Altogether, throughout the year, both species showed a positive energy balance, regarding the energy surplus available for somatic growth, gonads, and/or energy reserves (lipids) of the organisms (SfG'), though it was close to zero during spring in *P. anceps* (Fig. 7b). In general, the mean SfG' was higher in *P. anceps* than in *P. nutans*, which when assuming similar symbiont translocation and excretion losses in the species might reflect differences in growth rates, though no information is available for these species. Still, when comparing growth rates, *Plexaurella* spp. apparently exhibits much lower growth rates, compared to other Caribbean octocorals, which has been suggested to be a trade-off between elongation and thickening of branches, as this species also has the thickest branches (Yoshioka and Yoshioka 1991). Based on this assumption, the measured differences here in branch thickness of *P. anceps* and *P. nutans* (1.22 ± 0.2 and 1.59 ± 0.7 cm, respectively) might indicate a higher growth rate of the former species. However, the difference in the seasonal pattern could also be related to differences in reproduction periods of the species.

So far, information on reproductive mode and timing in the studied octocorals are based on single observations, with *P. anceps* seemingly reproducing by brooding embryos at the colony surface (Ritson-Williams 2010), while broadcast spawning has been reported for *P. nutans* (Kahng et al. 2011). Also, according to these studies, the timing of reproduction differs between the species, as *P. anceps* has been found brooding during autumn (October), while spawning in *P. nutans* has been reported in summer (July). This could explain the differences in seasonal patterns, regarding the energy surplus that can be used for growth, as well as for reproduction, as the seasonally highest SfG' in both species was found in the reported respective reproduction periods (Fig. 7).

Implications for benthic–pelagic coupling in the reef lagoon

The clear differences in prey capture (higher in *P. anceps* than *P. nutans*) suggest a higher efficiency in polyp prey

capture capability of *P. anceps*. As the two species did not show significant differences in their colony biometry, regarding branching patterns and length and number of branches, this may be related to differences in the flexibility of the colonies (Sponaugle and LaBarbera 1991), their polyp morphology (Dai and Lin 1993), and/or the density (and efficiency) of the nematocysts (Östman 1989; Purcell and Mills 1989). Also, in the study area, while having similar colony densities ($0.047 \pm 0.004 \text{ m}^{-2}$ and $0.058 \pm 0.003 \text{ m}^{-2}$ for *P. anceps* and *P. nutans*, respectively; Padilla, pers. comm.), *P. anceps* colonies occur in dense patches, while *P. nutans* colonies are more uniformly distributed (Rossi, pers. obs.), which may have a direct effect on the prey capture rates due to the higher retention of the near-bottom seston within the patch (Guizien and Ghisalberti 2017). The patchiness of the *P. anceps* colonies and their high flexibility that might reduce flow velocity and turbulence at the polyp level could result in a higher retention of particles and potential zooplankton preys (Sponaugle and LaBarbera 1991; Wildish and Kristmanson 1997; Riisgard and Larsen 2017). In contrast, the wider distance between *P. nutans* colonies and their relative stiffness may lower the capacity of the species to retain particles. This hypothesis was supported by the mean annual zooplankton removal rate of the species of 0.0162 ± 0.03 and $0.0061 \pm 0.012 \text{ mg C m}^{-2} \text{ day}^{-1}$ for *P. anceps* and *P. nutans*, respectively, based on species' heterotrophic carbon ingestion per polyp, polyp number per colony, and colony density in the reef lagoon. This was comparable with the removal of $0.15 \text{ mg C m}^{-2} \text{ d}^{-1}$ reported in the Caribbean *E. flexuosa*, when considering the tenfold higher colony density of this species ($0.45 \text{ colonies m}^{-2}$; Ribes et al. 1998).

Critical considerations and future research

This work represents one of a few that have simultaneously studied the autotrophic and heterotrophic seasonal inputs of benthic suspension feeders, providing key information for understanding the balance between autotrophic and heterotrophic inputs, as well as their variability. The ability of corals to modulate their feeding modes under different environments may provide an adaptive mechanism to sustain growth under stressful conditions. This knowledge is of increasing importance, considering that climate change and local impacts are drastically changing the energy fluxes in coastal areas (Rossi et al. 2019a) and will help explain the already observed (reviewed in Schubert et al. 2017) and predicted potential near-future transformation of the seascape in coral reefs and other marine animal forests (sensu Rossi et al. 2017a).

Hence, the accurate assessment of contributions of autotrophic and heterotrophic energy inputs, their

variations (flexibility), and the associated carbon fluxes is of great importance. However, we are still greatly lacking key information to obtain more accurate estimations, as for the calculation in this and many other previous studies, assumptions are made, especially considering the heterotrophic contributions. For example, for the estimations of heterotrophic carbon assimilation by the two gorgonians studied here, two assumptions were made that require more detailed future studies to obtain more exact values for the carbon fluxes related to these benthic suspension feeders. The first was regarding the prey digestion time that is essential to evaluate the gut contents in cnidarians (Purcell 1983; Coma et al. 1994; Rossi et al. 2004). This factor has been shown to vary with temperature (Fig. S1), but we should also consider that there may be differences in the efficiency of organic matter assimilation between species (see Rossi et al. 2004; Coma et al. 2015). So far, only three studies have reported prey digestion times in temperate octocorals, but no data are available for tropical species. We cannot exclude that at higher temperatures in summer, prey may disappear from the gastric cavity of octocorals in less than the reported two hours in scleractinians (Table S1; Kuanui et al. 2016), hence, leading to an underestimation of both the kind of prey and the associated carbon (Rossi et al. 2012, but see Leal et al. 2014).

The second assumption is concerning the polyp activity that was assumed to be 24 h in this study, as no information is available for the studied species. Though, based on scarce studies on coral polyp activity rhythms, they seem to exhibit species-specific differences, with reports for Caribbean octocorals showing either only daytime or day- and nighttime activity (reviewed in Schubert et al. 2017). Polyp activity and the discontinuity of near-bottom seston abundance in short time periods are two of the most neglected pathways in benthic–pelagic coupling processes (Rossi et al., 2019b). Zooplankton is far from being present all the time, and its concentration is not at all homogeneous in coral reefs when considering daily cycles (Palardy et al. 2006). This means that when monitoring an annual cycle, with one monthly sampling, one is far from understanding the potential food pulses (discontinuous availability of prey items) present in the study area (Tsounis et al. 2006). Polyp activity is tightly related to current speed and zooplankton nutritional signals or the presence (Rossi et al. 2019b), so the capture rates will be proportional to both parameters that may change constantly during the day. Hence, there is a great need for a better understanding of the importance of these food pulses to more accurately quantifying the importance of heterotrophic inputs in reef organisms.

Also, regarding the comparison of the autotrophic contributions of the two studied species, a similar translocation from the algal symbionts to the host was assumed. On the one hand, this might be true, considering that the

Symbiodiniaceae of both species belong to the genus *Breviolum* (LaJeunesse et al. 2018), formerly known as clade B (reviewed in Franklin et al. 2012). On the other hand, the *Breviolum* species and, hence, proportion of photosynthetate translocated to the host may differ between *P. anceps* and *P. nutans*, as in the former, only one type (B1) has been reported, while the latter has shown to be associated with three different types (B1, B19, B1a) (reviewed in Franklin et al. 2012).

Acknowledgements We thank E. Escalante Mancera and F. G. Ruiz Rentería for providing light, SST, and water velocity data from the Oceanographically and Meteorological Monitoring Academic Service (SAMMO, Coral Reef Systems Academic Unit- UASA, ICMYL, UNAM). We also want to thank H. Absalón Yam Poot for his help with the laboratory work and Walter Rich for English editing. SR was funded with a Marie Curie International Outgoing Fellowship (ANIMAL FOREST HEALTH, Grant Agreement Number 327845) and P-SPHERE (COFUND Marie Curie, Grant Agreement Number 665919). MO Soares thanks the Conselho Nacional de Desenvolvimento Científico e Tecnológico—CNPq (Grant Numbers 233808/2014-0 and 307061/2017-5), CAPES PRINT Programme, and INCT AmbTropic for the financial support. The authors would like to thank the AGAUR Generalitat de Catalunya excellence program (MERS, 2017 SGR 1588). This work contributes to the ICTA María de Maetzu “Unit of Excellence” (MinECo, MDM2015-0552).

References

- Álvarez-Cadena JN, Ordóñez-López U, Almaral-Mendivil AR (2009) Composition and abundance of zooplankton groups from a coral reef lagoon in Puerto Morelos, Quintana Roo, Mexico, during an annual cycle. *Rev Biol Trop* 57:647–658
- Anthony KRN, Fabricius KE (2000) Shifting roles of heterotrophy and autotrophy in coral energetics under varying turbidity. *J Exp Mar Biol Ecol* 252:221–253
- Baker DM, Webster KL, Kim K (2010) Caribbean octocorals record changing carbon and nitrogen sources from 1862 to 2005. *Glob Change Biol* 16:2701–2710
- Baker DM, Freeman CJ, Knowlton N, Thacker RW, Kim K, Fogel ML (2015) Productivity links morphology, symbiont specificity, and bleaching in the evolution of Caribbean octocoral symbioses. *ISME J* 9:2620–2629
- Bednarz VN, Cardini U, van Hoytema N, Al-Rshaidat MMD, Wild C (2015) Seasonal variation in dinitrogen fixation and oxygen fluxes associated with two dominant zooxanthellate soft corals from the northern Red Sea. *Mar Ecol Prog Ser* 519:141–152
- Beers JR (1966) Studies on the chemical composition of the major zooplankton groups in the Sargasso Sea off Bermuda. *Limnol Oceanogr* 11:520–528
- Biswas AK, Biswas MR (1979) Handbook of environmental data and ecological parameters: environmental sciences and applications, vol 6. Pergamon, Oxford
- Cocito S, Ferrier-Pagès C, Cupido R, Rottier C, Meier-Augenstein W, Kemp H, Reynaud S, Peirano A (2013) Nutrient acquisition in four Mediterranean gorgonian species. *Mar Ecol Prog Ser* 473:179–188
- Coma R, Gili JM, Zabala M, Riera T (1994) Feeding and prey capture cycles in the aposymbiotic gorgonian *Paramuricea clavata*. *Mar Ecol Prog Ser* 115:257–270
- Coma R, Ribes M, Gili JM, Zabala M (1998) An energetic approach to the study of life-history traits of two modular colonial benthic invertebrates. *Mar Ecol Prog Ser* 162:89–103
- Coma R, Llorente-Llurba E, Serrano E, Gili JM, Ribes M (2015) Natural heterotrophic feeding by a temperate octocoral with symbiotic zooxanthellae: a contribution to understanding the mechanisms of die-off events. *Coral Reefs* 34(2):549–560
- Coppari M, Gori A, Viladrich N, Saponari L, Grinyó J, Olariaga A, Rossi S (2016) The role of sponges in the benthic-pelagic coupling process in warm temperate coastal bottoms. *J Exp Mar Biol Ecol* 477:57–68
- Coppari M, Zanella C, Rossi S (2019) The importance of coastal gorgonians in the blue carbon budget. *Sci Rep* 9(1):1–12
- Crandall JB (2014) Sun and symbionts: translocation in Caribbean corals. Ph.D. thesis, State University of New York, p 232
- Dai C-F, Lin MC (1993) The effects of flow on feeding of three gorgonians from southern Taiwan. *J Exp Mar Biol Ecol* 173:57–69
- Elias-Piera F, Rossi S, Gili JM, Orejas C (2013) Trophic ecology of seven Antarctic gorgonian species. *Mar Ecol Prog Ser* 477:93–106
- Enríquez S, Pantoja-Reyes NI (2005) Form-function analysis of the effect of canopy morphology on leaf self-shading in the seagrass *Thalassia testudinum*. *Oecologia* 145:235–243
- Fabricius KE, Klumpp DW (1995) Widespread mixotrophy in reef-inhabiting soft corals: the influence of depth, and colony expansion and contraction on photosynthesis. *Mar Ecol Prog Ser* 125:195–204
- Farrant PA, Borowitzka MA, Hinde R, King RJ (1987) Nutrition of the temperate Australian soft coral *Capnella gaboensis*. II: the role of zooxanthellae and feeding. *Mar Biol* 95:575–581
- Ferrier-Pagès C, Leal MC (2019) Stable isotopes as tracers of trophic interactions in marine mutualistic symbioses. *Ecol Evol* 9(1):723–740
- Ferrier-Pagès C, Reynaud S, Béraud E, Rottier C, Menu D, Duong G, Gévaert F (2015) Photophysiology and daily primary production of a temperate symbiotic gorgonian. *Photosynth Res* 12:95–104
- Franklin EC, Stat M, Pochon X, Putnam HM, Gates RD (2012) GeoSymbio: a hybrid, cloud-based web application of global geospatial bioinformatics and ecoinformatics for Symbiodinium–host symbioses. *Mol Ecol Res* 12:369–373
- Fry B, Sherr EB (1989) $\delta^{13}\text{C}$ measurements as indicators of carbon flow in marine and freshwater ecosystems. In: Rundel P (ed) Stable isotopes in ecological research. Springer, New York, pp 196–229
- Grottoli AG, Rodrigues LJ, Palardy JE (2006) Heterotrophic plasticity and resilience in bleached corals. *Nature* 440:1186–1189
- Guizien K, Ghisalberti M (2017) Living in the canopy of the animal forest: physical and biogeochemical aspects. In: Rossi S, Bramanti L, Gori A, Orejas C (eds) Marine animal forests: the ecology of benthic biodiversity hotspots. Springer, Switzerland, pp 507–528
- Hall DJ, Cooper WE, Werner EE (1970) An experimental approach to the production dynamics and structure of freshwater animal communities. *Limnol Oceanogr* 15:838–928
- Hobson KA, Welch HE (1992) Determination of trophic relationships within a high Arctic marine food web using $\delta^{13}\text{C}$ and $\delta^{15}\text{N}$ analysis. *Mar Ecol Prog Ser* 84(1):9–18
- Hughes TP, Barnes ML, Bellwood DR, Cinner JE, Cumming GS, Jackson JBC, Kleypas J, Leemput IAV, Lough JM, Morrison TH, Palumbi SR, Nes EV, Scheffer M (2017) Coral reefs in the Anthropocene. *Nature* 546:82–90
- Iglesias-Prieto R, Matta JL, Robins WA, Trench RK (1992) Photosynthetic response to elevated temperature in the symbiotic dinoflagellate *Symbiodinium microadriaticum* in culture. *Proc Natl Acad Sci* 89:10302–10305

- Jacob U, Mintenbeck K, Brey T, Knust R, Beyer K (2005) Stable isotope food web studies: a case for standardized sample treatment. *Mar Ecol Prog Ser* 287:251–253
- Jeffrey SW, Humphrey GF (1975) New spectrophotometric equations for determining chlorophylls *a*, *b*, *c*₁ and *c*₂ in higher plants, algae and natural phytoplankton. *Biochem Physiol Pflanzen* 167:191–194
- Jones CG, Lawton LH, Shachak M (1994) Organisms as ecosystem engineers. *Oikos* 69:373–376
- Jordán Dahlgren E (1989) Gorgonian community structure and reef zonation patterns on Yucatan coral reefs. *Bull Mar Sci* 45(3):678–696
- Kahn SE, Benayahu Y, Lasker HR (2011) Sexual reproduction in octocorals. *Mar Ecol Prog Ser* 443:265–283
- Kuanui P, Chavanich S, Viyakarn V, Park HS, Omori M (2016) Feeding behaviors of three tropical scleractinian corals in captivity. *Trop Zool* 29:1–9
- Kupfner Johnson SA (2019) Untapped potential of gorgonian octocorals for detecting environmental change in Biscayne National Park, Florida, USA. Ph.D. thesis, University of South Florida, p 290
- LaJeunesse TC, Parkinson JE, Gabrielson PW, Jeong HJ, Reimer JD, Voolstra CR, Santos SR (2018) Systematic revision of Symbiodiniaceae highlights the antiquity and diversity of coral endosymbionts. *Curr Biol* 28(16):2570–2580
- Land LS, Eustice RA, Lang JC, Macko SA (2000) Plankton-benthos coupling on a Caribbean fringing reef. In: Proceedings of 9th international coral reef symposium, vol 1, pp 101–106
- Leal MC, Nejstgaard JC, Calado R, Thompson ME, Frischer ME (2014) Molecular assessment of heterotrophy and prey digestion in zooxanthellate cnidarians. *Mol Ecol* 23:3838–3848
- McCauley M, Goulet TL (2019) Caribbean gorgonian octocorals cope with nutrient enrichment. *Mar Poll Bull* 141:621–628
- McConnaughey T, McRoy CP (1979) Food-web structure and the fractionation of carbon isotopes in the Bering Sea. *Mar Biol* 53(3):257–262
- Muscatine L, McCloskey IR, Marian RE (1981) Estimating the daily contribution of carbon from zooxanthellae to coral animal respiration. *Limnol Oceanogr* 26:601–611
- Muscatine L, Porter JW, Kaplan IR (1989) Resource partitioning by reef corals as determined from stable isotope composition. I. $\delta^{13}\text{C}$ of zooxanthellate and animal tissue versus depth. *Mar Biol* 100:185–193
- Nahon S, Richoux NB, Kolasinski J, Desmalades M, Ferrier-Pagès C, Lecellier G, Planes S, Berteaux Lecellier V (2013) Spatial and temporal variations in stable carbon ($\delta^{13}\text{C}$) and nitrogen ($\delta^{15}\text{N}$) isotopic composition of symbiotic scleractinian corals. *PLoS ONE* 8:e81247
- Östman C (1989) Nematocyst as taxonomic criteria in the family of Campanulariidae. In: Hessinger DA, Lenhoff HM (eds) The biology of nematocysts. University of California, Irvine, pp 501–518
- Owens NJP (1988) Natural variations in ^{15}N in the marine environment. *Adv Mar Biol* 24:389–451
- Palardy JE, Grotto AG, Matthews KA (2006) Effect of naturally changing zooplankton concentrations on feeding rates of two coral species in the Eastern Pacific. *J Exp Mar Biol Ecol* 331:99–107
- Pupier CA, Fine M, Bednarz VN, Rottier C, Grover R, Ferrier-Pagès C (2019) Productivity and carbon fluxes depend on species and symbiont density in soft coral symbioses. *Sci Rep* 9(1):1–10
- Purcell JE (1983) Digestion rates and assimilation efficiencies of siphonophores fed zooplankton prey. *Mar Biol* 73:257–261
- Purcell JE, Mills CE (1989) The correlation between nematocyst types and diet in pelagic Hydrozoa. In: Hessinger DA, Lenhoff HM (eds) The biology of nematocysts. University of California, Irvine, pp 463–486
- Ramsby BD, Shirur KP, Iglesias-Prieto R, Goulet TL (2014) *Symbiodinium* photosynthesis in Caribbean octocorals. *PLoS ONE* 9(9):e106419
- Ribes M, Coma R, Gili JM (1998) Heterotrophic feeding by gorgonian corals with symbiotic zooxanthella. *Limnol Oceanogr* 43:1170–1179
- Ribes M, Coma R, Gili JM (1999) Heterogeneous feeding in benthic suspension feeders: the natural diet and grazing rate of the temperate gorgonian *Paramuricea clavata* (Cnidaria: Octocorallia) over a year cycle. *Mar Ecol Prog Ser* 183:125–137
- Riisgard HU, Larsen OS (2017) Filter-feeding zoobenthos and hydrodynamics. In: Rossi S, Bramanti L, Gori A, Orejas C (eds) Marine Animal Forests: the ecology of benthic biodiversity hotspots. Springer, Switzerland, pp 787–812
- Ritson-Williams R (2010) Surface brooding in the Caribbean gorgonian *Pterogorgia anceps*. *Coral Reefs* 29:437
- Rossi S, Ribes M, Coma R, Gili JM (2004) Temporal variability in zooplankton prey capture rate of the passive suspension feeder *Leptogorgia sarmentosa* (Cnidaria: Octocorallia), a case study. *Mar Biol* 144(1):89–99
- Rossi S, Gili JM, Coma R, Linares C, Gori A, Vert N (2006) Temporal variation in protein, carbohydrate, and lipid concentrations in *Paramuricea clavata* (Anthozoa, Octocorallia): evidence for summer-autumn feeding constraints. *Mar Biol* 149:643–651
- Rossi S, Bramanti L, Broglio E, Gili JM (2012) Trophic impact of long-lived species indicated by population dynamics in a short-lived hydrozoan *Eudendrium racemosum*. *Mar Ecol Prog Ser* 467:97–111
- Rossi S, Bramanti L, Gori A, Orejas C (2017a) An overview of the animal forests of the world. In: Rossi S, Bramanti L, Gori A, Orejas C (eds) Marine animal forests: the ecology of benthic biodiversity hotspots. Springer, Switzerland, pp 1–28
- Rossi S, Coppari M, Viladrich N (2017b) Benthic-pelagic coupling: new perspectives in the animal forests. In: Rossi S, Bramanti L, Gori A, Orejas C (eds) Marine animal forests: the ecology of benthic biodiversity hotspots. Springer, Switzerland, pp 855–886
- Rossi S, Schubert N, Brown D, Soares MO, Grosso V, Rangel-Huerta E, Maldonado E (2018) Linking host morphology and symbiont performance in octocorals. *Sci Rep* 8:12823
- Rossi S, Isla E, Bosch-Belmar M, Galli G, Gori A, Gristina M, Ingrosso G, Milisenda G, Piraino S, Rizzo L, Schubert N, Soares MO, Solidoro C, Thurstan RH, Viladrich N, Willis TJ, Ziveri P (2019a) Changes of energy fluxes in marine animal forests of the Anthropocene: factors shaping the future seascape. *ICES J Mar Sci* 76(7):2008–2019
- Rossi S, Rizzo L, Duchêne JC (2019b) Polyp expansion of passive suspension feeders: a red coral case study. *PeerJ* 7:e7076
- Schlichter D, Svoboda A, Kremer BP (1983) Functional autotrophy of *Heteroxenia fuscescens* (Anthozoa: Alcyonaria): carbon assimilation and translocation of photosynthates from symbionts to host. *Mar Biol* 78:29–38
- Schubert N, Brown D, Rossi S (2017) Symbiotic versus non-symbiotic octocorals: physiological and ecological implications. In: Rossi S, Bramanti L, Gori A, Orejas C (eds) Marine animal forests: the ecology of benthic biodiversity hotspots. Springer, Switzerland, pp 887–918
- Sebess KP, Koehl MAR (1984) Predation on zooplankton by the benthic anthozoans *Alcyonium siderium* (Alcyonacea) and *Metridium senile* (Actiniaria) in the New England subtidal. *Mar Biol* 81(3):255–271
- Slaterry M, McClintock JB (1995) Population structure and feeding deterrence in three shallow-water Antarctic soft corals. *Mar Biol* 122:461–470
- Sorokin YI (1991) Biomass, metabolic rates and feeding of some common reef zoantharians and octocorals. *Aust J Mar Freshw Res* 42:729–741

- Sponaugle S, LaBarbera M (1991) Drag-induced deformation: a functional feeding strategy in two species of gorgonians. *J Exp Mar Biol Ecol* 148:121–134
- Tsounis G, Rossi S, Laudien J, Bramanti L, Fernández N, Gili JM, Arntz W (2006) Diet and seasonal prey capture rates in the Mediterranean red coral (*Corallium rubrum* L.). *Mar Biol* 149:313–325
- Ward-Paige CA, Risk MJ, Sherwood OA (2005) Reconstruction of nitrogen sources on coral reefs: $\delta^{15}\text{N}$ and $\delta^{13}\text{C}$ in gorgonians from Florida Reef Tract. *Mar Ecol Prog Ser* 296:155–163
- Wildish D, Kristmanson D (1997) Benthic suspension feeders and flow. Cambridge University Press, Cambridge
- Yoshioka PM, Yoshioka BB (1991) A comparison of the survivorship and growth of shallow-water gorgonian species of Puerto Rico. *Mar Ecol Prog Ser* 69:253–260

Publisher's Note Springer Nature remains neutral with regard to jurisdictional claims in published maps and institutional affiliations.